large number of states arise from coupling the d^5 core to the pyrazine anion within the dimer. It seems more appropriate to concentrate on the low-energy transitions that are so unique to the C–T mixed-valence ion.

In the <6000-cm^{-1} energy region our MCD data have unveiled a broad (YZ-) polarized transition extending beyond the range of our current instrumentation. Structure and X intensity within the 6400-cm^{-1} system are also not envisaged by current models, and we are forced to consider both the contribution of electronic structure within the $t_2{}^5$ basis of the dimer system and vibronic activity (involvement of nontotally symmetric modes of vibration that change the overall symmetry of an electronic vibrational state).

Starting from a basis consisting of Ru^{2+} with its filled $t_2{}^6$ configuration and Ru^{3+} as basically a hole in this filled shell, it is clear that electronic splittings of the order of 1000 cm^{-1} must originate in the structure of the $t_2{}^5$ configuration. Vibrational energies are also in the range 200–2000 cm^{-1}. The e_g orbitals on the metal and the π^* orbitals on the ligand are clearly well separated in energy from the t_2 orbitals. The effects of spin–orbit coupling and low symmetry will split the $t_2{}^5$ configuration into three Kramers doublets. Upon introduction of an interaction between the two centers and formation of states consistent with the observed equivalence of the two ruthenium centers, six levels will ensue, three gerade and three ungerade. In the most general case, three electric dipole allowed transitions would be expected with energy separations of the order of the spin–orbit splitting on Ru^{3+} and the specific interion interaction energy. The inclusion of vibronic coupling could then be envisaged in a manner analogous to that used by Piepho, Krausz, and Schatz.[10] Such an analysis is in progress.[11]

Our deuteration results indicate that the high-energy shoulder is most likely a vibrational sideband system of the stronger pure electronic region at lower energy that does not shift on deuteration. As noted the MCD result precludes this being a simple Franck–Condon coupling to a totally symmetric mode, and we conclude that vibronic activity is present but not dominant.

The mystery of the Creutz–Taube ion seemingly originates in a fine balance between the specific interaction between the two metal centers, the back-bonding character of Ru^{2+}, the weak forward bonding of Ru^{3+} toward the pyrazine ligand, and the spin–orbit and low-symmetry fields that may tend to reduce vibronic effects. A simple model concentrating on the electronic coupling has been formulated by Dubicki, Ferguson, and Krausz.[12] Comparison with experiment is somewhat limited by lack of data in the region below 4000 cm^{-1} where the third electronically allowed dimer feature is expected. These low-energy features are primarily due to the Ru^{3+} single ion. Measurements on other strongly interacting mixed-valence dimers are also necessary. We are working toward both these goals.

Acknowledgment. E.K. acknowledges the assistance of Dr. R. J. Robbins in programming the Kramers–Kronig transform of the reflectance data and helping at all phases of data processing. The help and encouragement of Dr. J. Ferguson at all phases of this work have been essential. Some initial MCD measurements were done in collaboration with Dr. H. U. Guedel and performed at the University of Virginia with support from Prof. P. N. Schatz. There have been many fruitful discussions with Dr. L. Dubicki and Dr. S. B. Piepho.

Registry No. [II,II]$(ZnCl_4)_2$, 87922-19-8; [II,III]Cl_5, 94780-98-0; [II,III]$(tos)_5$, 41557-38-4; [III,III]Cl_6, 94750-87-5.

---

(11) Schatz, P. N.; Neuenschwander, K., personal communication.

(12) Dubicki, L.; Krausz, E. R.; Ferguson, J., submitted for publication in *J. Am. Chem. Soc.*

Contribution from the Institut für Anorganische Chemie
and Laboratorium für Kristallographie, Universität Bern, CH-3000 Bern 9, Switzerland

The Creutz–Taube Complex Revisited: Crystallographic Study of the Electron-Transfer Series $[(NH_3)_5Ru(pyz)Ru(NH_3)_5]^{n+}$ (n = 4–6)

URS FÜRHOLZ,[1a] STEFAN JOSS,[1a] HANS BEAT BÜRGI,*[1b] and ANDREAS LUDI*[1a]

Received May 9, 1984

The crystal and molecular structures of the following four compounds have been determined: $[(NH_3)_5Ru(pyz)Ru(NH_3)_5](ZnCl_4)_2$ (pyz = pyrazine), [II,II], orthorhombic, *Pcab*, a = 11.348 (2) Å, b = 11.614 (2) Å, c = 22.144 (3) Å, Z = 4, R = 2.5% for 2178 reflections; $[(NH_3)_5Ru(pyz)Ru(NH_3)_5]Cl_5\cdot5H_2O$, [II,III], orthorhombic, *Pnnm*, a = 17.595 (2) Å, b = 11.308 (2) Å, c = 7.021 (1) Å, Z = 2, R = 2.4% for 1023 reflections; [II,III]$(tos)_5\cdot4H_2O$ (100 K, tos = p-toluenesulfonate), triclinic, $P\bar{1}$, a = 13.162 (3) Å, b = 15.116 (5) Å, c = 15.749 (5) Å, α = 106.96 (2)°, β = 94.40 (2)°, γ = 103.15 (2)°, Z = 2, R = 3.2% for 5304 reflections; $[(NH_3)_5Ru(pyz)Ru(NH_3)_5]Cl_6\cdot2H_2O$, [III,III], monoclinic, $P2_1/n$, a = 7.465 (2) Å, b = 11.401 (2) Å, c = 14.613 (2) Å, β = 79.60 (2)°, Z = 2, R = 2% for 2503 reflections. Important average distances are in the order [II,II}, [II,III], [III,III]: Ru–N(pyz) = 2.013 (3), 1.991 (9), 2.15 (1) Å; Ru–NH_3(trans) = 2.149 (3), 2.123 (7), 2.089 (1) Å; Ru–NH_3(cis) = 2.132 (3), 2.112 (3), 2.101 (5) Å; C–N = 1.353 (4), 1.362 (4), 1.341 (2) Å; C–C = 1.363 (5), 1.361 (5), 1.382 (2) Å. The overall geometries of the binuclear ions in all four compounds are very similar and are adequately described by an eclipsed arrangement of the two mononuclear subunits, with the pyrazine plane bisecting the *cis*-Ru–NH_3 bonds. The geometry of the [II,III] ion cannot be explained as the average of the geometries of [II,II] and [III,III]. The crystallographic results are compatible with two equivalent ruthenium atoms in the mixed-valence ion and demonstrate the significance of the ruthenium–pyrazine, t_{2g}–π^* bonding.

Introduction

Current models[2] for mixed-valence compounds distinguish between two limiting situations: class II or localized vs. class III or delocalized. The first case corresponds to a two-minima energy surface, a classical example is Prussian Blue with only weak coupling between Fe(II) and Fe(III). The second case corresponds to a single-minimum potential. Intermediate cases are represented by double-minimum wells with a separating barrier on the order of or smaller than thermal energy. These models have been extended by Schatz and co-workers (PKS model[3]) by introducing vibronic and electronic coupling between the two Ru subunits. Their description extracts the relevant model parameters by fitting position, intensity, and shape of the intervalence band to the experimental data. Let us emphasize that these models do not take into account the electronic structure of the bridging ligand

---

(1) (a) Institut für Anorganische Chemie. (b) Laboratorium für Kristallographie.

(2) Robin, M. B.; Day, P. *Adv. Inorg. Chem. Radiochem.* **1967**, *10*, 247. Hush, N. S. *Prog. Inorg. Chem.* **1967**, *8*, 391.

(3) Wong, K. Y.; Schatz, P. N. *Prog. Inorg. Chem.* **1981**, *28*, 369.

0020-1669/85/1324-0943$01.50/0 © 1985 American Chemical Society

Table I. Crystal Data for $[II,II](ZnCl_4)_2$, $[II,III]Cl_5{\cdot}5H_2O$, $[II,III](tos)_5{\cdot}4H_2O$, and $[III,III]Cl_6{\cdot}2H_2O$

	$[II,II](ZnCl_4)_2$	$[II,III]Cl_5{\cdot}5H_2O$	$[II,III](tos)_5{\cdot}4H_2O$		$[III,III]Cl_6{\cdot}2H_2O$
T, K	295	295	295	100	295
no. of reflcns for unit cell determin	25	14	14	20	16
θ range, deg	10-16	16-18	11-13	10-16	11-23
space gp	*Pcab*	*Pnnm*	$P\bar{1}$	$P\bar{1}$	$P2_1/n$
a, Å	11.348 (2)	17.595 (2)	13.267 (3)	13.162 (3)	7.465 (2)
b, Å	11.614 (2)	11.308 (2)	15.401 (4)	15.116 (5)	11.401 (2)
c, Å	22.144 (3)	7.021 (1)	15.793 (8)	15.749 (5)	14.613 (2)
α, deg			107.81 (3)	106.96 (2)	
β, deg			94.15 (3)	94.40 (2)	79.60 (2)
γ, deg			103.99 (2)	103.15 (2)	
V, Å^3	2918.6 (14)	1397.1 (6)	2943.3 (50)	2883.9 (33)	1223.2 (5)
Z	4	2	2	2	2
fw	866.9	719.9	1380.5	1380.5	683.3
D_{measd}(flotation), g cm^{-3}	1.97 (2)	1.71 (2)	1.56 (2)		1.86 (2)
D_{calcd}, g cm^{-3}	1.973	1.711	1.559	1.579	1.855

Chart I[a]

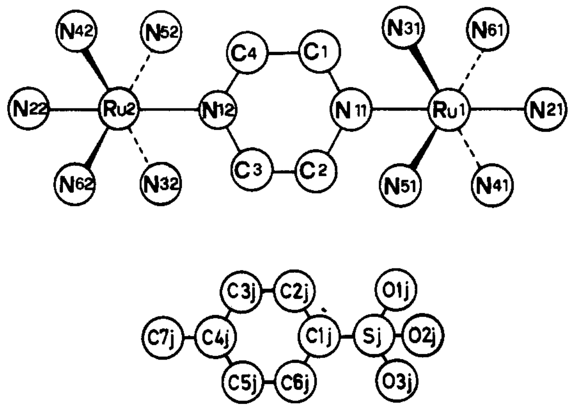

[a] Numbering of atoms for symmetric dimers: Ru2 = Ru1 = Ru; C4 = C2; C3 = C1; Nj1 = Nj2 = Nj; Oj = lattice water.

explicitly. Also, the properties of the monovalent mononuclear subunits are used as points of reference rather than those of the reduced and oxidized dimers.

In a recent review on mixed-valence d^6–d^5 complexes[4] it was concluded that the (μ-pyrazine)decaamminediruthenium(II,III) ion, the Creutz–Taube ion (Chart I), is close to the limiting case "delocalized". A reexamination and redetermination of some relevant physical properties of this prototype mixed-valence complex led to the conclusion that the interaction between the d orbitals of the metal centers and the π orbitals of the briding ligand is a crucial factor indeed for the discussion of its electronic structure.[5] This strong interaction between Ru(II) and π-accepting ligands such as pyrazine plays a key role in the coordination chemistry of ruthenium.[6] In the course of a collaborative reinvestigation of the Creutz–Taube ion[5] we performed a crystallographic study of the complete electron-transfer series, i.e. of the three binuclear species $[(NH_3)_5Ru(pyz)Ru(NH_3)_5]^{4+}$ = [II,II], $[(NH_3)_5Ru(pyz)Ru(NH_3)_5]^{5+}$ = [II,III], and $[(NH_3)_5Ru(pyz)Ru(NH_3)_5]^{6+}$ = [III,III], where pyz = pyrazine. This paper reports the structural results and briefly discusses their relevance to the electronic properties of the mixed-valence ion.

Experimental Section

A. Preparations. All the preparations were carried out under argon with Schlenk glassware.

$[(NH_3)_5Ru(pyz)Ru(NH_3)_5](ZnCl_4)_2$, $[II,II](ZnCl_4)_2$. A slurry of 3.0 g of $[Ru(NH_3)_5Cl]Cl_2$ in 50 mL of 10^{-4} M HCl was reduced with freshly prepared Zn/Hg (2 h). After addition of pyrazine (0.4 g) the resulting purple solution was transferred to another Schlenk vessel and kept in the dark for 6 h. A total of 20 mL of 4 M $ZnCl_2$ was added, and the resulting mixture was cooled to 0 °C for 0.5 day. The crystalline, dark purple precipitate was collected by filtration, washed with small portions of ethanol and ether, and vacuum dried; yield 3.2 g of $[II,II](ZnCl_4)_2$ (80%). Anal. Calcd: Ru, 23.3; C, 5.5; H, 4.0; N, 19.4; Cl, 32.7. Found: Ru, 23.7; C, 5.4; H, 4.1; N, 19.5; Cl, 32.3.

$[(NH_3)_5Ru(pyz)Ru(NH_3)_5]Cl_6{\cdot}2H_2O$, $[III,III]Cl_6{\cdot}2H_2O$. A solution of 2 g of $[II,II](ZnCl_4)_2$ in 100 mL of 0.1 M HCl was slowly oxidized by bubbling Cl_2. The end of the reaction was indicated by a brandy color of the solution. Excess chlorine was removed in a rotating evaporator at 25 °C, and the solution was concentrated until a yellow-brown product began to precipitate. Precipitation was completed by cooling to 0 °C. The solid was collected on a glass frit, washed with ethanol and ehter, and vacuum dried; yield 1.0 g of $[III,III]Cl_6{\cdot}2H_2O$ (60%). Anal. Calcd: Ru, 28.8; C, 6.9; H, 5.4; N, 24.0; Cl, 30.4. Found: Ru, 29.7; C, 6.5; H, 5.4; N, 23.3; Cl, 30.0.

$[(NH_3)_5Ru(pyz)Ru(NH_3)_5]Cl_5{\cdot}5H_2O$, $[II,III]Cl_5{\cdot}5H_2O$. A 1-g sample of $[II,II](ZnCl_4)_2$ was slowly oxidized with Cl_2 as in the previous preparation. When the oxidation was complete, 1 g of $[II,II](ZnCl_4)_2$ was added. Owing to the large equilibrium constant (4×10^6) of the reaction $[II,II] + [III,III] \rightleftarrows 2[II,III]$, the mixed-valence complex was formed quantitatively. The solid compound was precipitated by adding 20 mL of a saturated aqueous LiCl solution and subsequent dropwise addition of ethanol–ether (2:1). The crystalline, dark purple precipitate was filtered, washed with ethanol and ether, and vacuum dried; yield 1.4 g of $[II,III]Cl_5{\cdot}5H_2O$ (85%). Anal. Calcd: Ru, 28.1; C, 6.7; H, 6.1; N, 23.4; Cl, 24.6. Found: Ru, 28.8; C, 6.8; H, 5.9; N, 22.9; Cl, 24.5.

$[II,III](tos)_5{\cdot}4H_2O$ (tos = p-Toluenesulfonate). This salt was produced by adding a saturated aqueous solution of Na(tos) to a solution of 1 g of $[II,III]Cl_5{\cdot}5H_2O$ in 100 mL of water. The solid precipitate was isolated, washed, and dried as above; yield 1.8 g of $[II,III](tos)_5{\cdot}4H_2O$ (95%). Anal. Calcd: Ru, 14.7; C, 33.9; H, 5.6; N, 12.2; S, 11.6. Found: Ru, 16.0; C, 33.8; H, 5.6; N, 12.1; S, 11.7.

Ru was analyzed spectrophotometrically.[7] Elemental analyses were performed by Ciba Geigy, Basel.

Crystal Growth. For $[II,II](ZnCl_4)_2$, $[II,III]Cl_5{\cdot}5H_2O$, and $[III,III]Cl_6{\cdot}2H_2O$ the following procedure was applied: An aqueous solution of the complex saturated at 30 °C was filtered through a Millipore filter. A tightly stoppered bottle with this solution was placed in a Dewar flask containing water of 30 °C. Slow cooling in a refrigerator produced crystals of up to 1-mm edge within 2 days. Crystals of $[II,III](tos)_5{\cdot}4H_2O$ with very irregular and rounded shapes were obtained by slow evaporation of a saturated aqueous solution in a desiccator over $CaCl_2$.

B. Collection and Reduction of Diffraction Data. The space group for each of the compounds was determined from the systematic extinctions observed on precession and Weissenberg photographs. Lattice constants (Table I) and intensities were measured on a CAD-4 diffractometer using Mo Kα radiation (graphite monochromator, λ = 0.71069 Å). Details of data collection and refinement are summarized in Table II. For all of the crystals three check reflections recorded every 120 min did not show systematic intensity fluctuations. Intensities were corrected for Lorentz-polarization effects and for absorption.[8] No absorption correction was applied for $[II,III](tos)_5{\cdot}4H_2O$. Neutral-atom scattering factors were chosen with anomalous dispersion corrections for Ru, Zn, Cl, O, N, and C.[9] Calculations were performed on a PDP 11/34 by

---

(4) Creutz, C. *Prog. Inorg. Chem.* **1983**, *30*, 1.

(5) Fürholz, U.; Bürgi, H. B.; Wagner, F. E.; Stebler, A.; Ammeter, J. H.; Krausz, E.; Clark, R. J. H.; Stead, M. J.; Ludi, A. *J. Am. Chem. Soc.* **1984**, *106*, 121.

(6) Taube, H. *Surv. Prog. Chem.* **1973**, *6*, 1.

(7) Marshall, E. D.; Rickard, R. R. *Anal. Chem.* **1950**, *22*, 795. Woodhead, J. L.; Fletcher, J. M. *J. Chem. Soc.* **1961**, 5039.

(8) Coppens, P.; Leiserowitz, L.; Rabinovich, D. *Acta Crystallogr.* **1965**, *18*, 1035.

(9) "International Tables for X-Ray Crystallography"; Kynoch Press: Birmingham, England, 1974.

Table II. Intensity Collection and Refinement for $[II,II](ZnCl_4)_2$, $[II,III]Cl_5 \cdot 5H_2O$, $[II,III](tos)_5 \cdot 4H_2O$, and $[III,III]Cl_6 \cdot 2H_2O$

	$[II,II](ZnCl_4)_2$	$[II,III]Cl_5 \cdot 5H_2O$	$[II,III](tos)_5 \cdot 4H_2O$	$[III,III]Cl_6 \cdot 2H_2O$
T, K	295	295	100	295
cryst faces	(100), $(\bar{1}00)$, (010), $(0\bar{1}0)$, (001), $(00\bar{1})$	(010), $(0\bar{1}0)$, (310), $(\bar{3}10)$, $(00\bar{1})$, (102)		(101), $(10\bar{1})$, (001), $(00\bar{1})$, (011), $(01\bar{1})$, $(0\bar{1}1)$, $(0\bar{1}\bar{1})$
cryst vol, mm^3	1.14×10^{-3}	0.9×10^{-3}	1×10^{-3} [a]	2.05×10^{-3}
lin abs coeff, cm^{-1}	38.22	15.74	7.63	18.75
range of transmissn factors	0.61–0.87	0.82–0.94		0.79–0.91
2θ limits, deg	1–56	1–56	1–46	1–56
scan width, deg	$0.8 + 0.35 \tan \theta$	$0.8 + 0.35 \tan \theta$	$1.3 + 0.35 \tan \theta$	$0.9 + 0.35 \tan \theta$
no. of unique reflcns measd	3572 ($+h,+k,+l$)	1478 ($+h,+k,+l$)	7657 ($\pm h,\pm k,+l$)	3056 ($\pm h,+k,+l$)
no. of unique reflcns with $I > 2\sigma(I)$	2178	1023 [b]	5304	2503
no. of parameters	232	133	903	207
w in least squares	$1/\sigma^2(I)$	$1/\sigma^2(I)$	$1/\sigma^2(I)$	$1/\sigma^2(I)$
R, %	2.5	2.4	3.2	2.0
R_w, %	2.4	2.4	2.9	2.3
goodness of fit	1.34	1.90		1.90

[a] Irregular shape, see section on crystal growth. [b] Number of reflections with $I > \sigma(I)$.

using versions 17 and 18 of the structure determination package (SDP) of Enraf-Nonius and on an IBM 3033 using the SHELX and XRAY 76 program system. The low-temperature attachment of Enraf-Nonius was employed for measuring the intensities of $[II,III](tos)_5 \cdot 4H_2O$ at 100 K, cooling the crystal with a cold stream of N_2. In order to minimize icing of the crystal the humidity was kept below 10% by placing silica gel underneath the lid of the diffractometer. The diffractometer housing was sealed with a polyethylene cover equipped with drybox gloves.

C. Solution and Refinement of the Structures. For $[II,III]Cl_5 \cdot 5H_2O$ the refinement started from the known crystal structure of $[II,III]Br_{10/3}Cl_{5/3} \cdot 4H_2O$ where Br and Cl were assumed disordered among seven fourfold positions with refined populations ranging from 0.03 to 0.963 (O was not identified).[10] Adapting this model to the pure chloride salt and refining populations led to R = 3.5%. However, the narrow reflection profiles seemed indicative of a rather well-ordered structure. Standard N–H···O, N–H···Cl, O–H···Cl, and O–H···O hydrogen-bond lengths served as a guide to assign Cl and O to specific positions and to develop a model of disorder in which populations are fixed (1, 0.5, 0.25). This model for which the number of variables is reduced by about 20 refined to R = 2.4%, a significant improvement that corroborates the assumed distinction between anion and water sites. The other structures were solved by Patterson and Fourier methods. ΔF maps calculated after anisotropic least-squares refinement of all of the non-hydrogen atoms revealed most of the hydrogen positions. For $[II,II](ZnCl_4)$ large temperature factors of the Cl atoms indicated disordered $ZnCl_4$ tetrahedra. Splitting of the chlorine atoms into two slightly different positions and constraining their population parameter produced a significant improvement. Hydrogen positions were calculated for the H atoms attached to the pyrazine and tosylate rings in $[II,III](tos)_5 \cdot 4H_2O$, assuming C–H = 0.95 Å. Independent refinement of positional and individual thermal parameters of the hydrogen atoms was carried out for $[II,II](ZnCl_4)_2$ and $[III,III]Cl_6 \cdot 2H_2O$. For $[II,III]Cl_5 \cdot 5H_2O$ and $[II,III](tos)_5 \cdot 4H_2O$ isotropic thermal parameters were refined collectively for similar groups of hydrogen atoms, i.e. H(pyz), $H(NH_3)$, H(tos), $H(CH_3)$, and $H(H_2O)$. The final shift/error was generally smaller than 0.01 and ΔF maps after convergence of the refinement showed chemically insignificant residual electron densities of less than 0.3 e/$Å^3$ outside the Ru atoms. The final atomic coordinates are given in Tables III–VI. Tables of thermal parameters, hydrogen positions, and the interatomic distances and angles for the tosylate and $ZnCl_4^{2-}$ anions as well as listings of structure factors and stereoviews of the unit cells are available as supplementary material.

Description of the Molecular Structures

Figure 1 shows a stereoview of the binuclear ion of $[II,III]Cl_5 \cdot 5H_2O$, a representative example of the symmetric dimer, also displaying the essential geometrical features for the [II,II] and [III,III] ions. The asymmetric [II,III] of $[II,III](tos)_5 \cdot 4H_2O$ is shown in Figure 2. For all three combinations of oxidation states the binuclear complexes show an eclipsed or almost eclipsed conformation of the two pseudooctahedral RuN_6 fragments (Table VII). For the noncentrosymmetric $[II,III](tos)_5 \cdot 4H_2O$ the deviation from the eclipsed geometry is 11°. Ideally the angle between the pyrazine plane and the *cis*-Ru–NH_3 bonds is 45°, as in $[II,III]Cl_5 \cdot 5H_2O$. For $[II,II](ZnCl_4)_2$, $[II,III](tos)_5 \cdot 4H_2O$, and $[III,III]Cl_6 \cdot 2H_2O$ the following angles are observed: 52 and 41°; 46, 47, 51, and 42°; 44 and 47°.

Planarity is imposed on the pyrazine ring by space group symmetry for $[II,III]Cl_5 \cdot 5H_2O$. No deviations from planarity exceeding the standard deviations of the atomic coordinates occur for [II,II] and [III,III]. Displacements up to 0.05 Å from the least-squares plane of the ring are observed for the triclinic tosylate salt of [II,III]. A similar situation is observed for the Ru–pyz–Ru fragment, where again space group symmetry forces a perfectly planar geometry for $[II,III]Cl_5 \cdot 5H_2O$. The ruthenium atom

Table III. Final Atomic Positional Parameters with Standard Deviations in Parentheses for $[II,II](ZnCl_4)_2$ [a]

atom	x	y	z
Ru	0.18888 (2)	0.04572 (2)	0.11902 (1)
N1	0.0785 (2)	0.0178 (2)	0.0494 (1)
N2	0.3049 (3)	0.0810 (3)	0.1935 (1)
N3	0.1043 (3)	−0.0857 (3)	0.1708 (2)
N4	0.2752 (3)	0.1775 (3)	0.0686 (1)
N5	0.0689 (3)	0.1659 (3)	0.1578 (1)
N6	0.3154 (3)	−0.0713 (3)	0.0839 (2)
C1	0.0583 (3)	−0.0866 (3)	0.0248 (2)
C2	0.0170 (3)	0.1036 (3)	0.0223 (2)
Zn	0.32757 (4)	0.01364 (4)	0.86602 (2)
Cl1	0.4292 (1)	0.9069 (1)	0.93410 (5)
Cl2	0.2232 (1)	0.8834 (1)	0.80992 (5)
Cl3	0.4531 (2)	0.1090 (2)	0.80463 (8)
Cl4	0.1974 (4)	0.1336 (5)	0.9004 (3)
Cl5	0.4204 (8)	0.9089 (7)	0.9430 (3)
Cl6	0.201 (2)	0.909 (2)	0.825 (1)
Cl7	0.4617 (2)	0.0954 (3)	0.8048 (1)
Cl8	0.2180 (2)	0.1478 (2)	0.91281 (8)

[a] Chlorine atoms have populations of 0.5.

Table IV. Final Atomic Positional Parameters with Standard Deviations in Parentheses for $[II,III]Cl_5 \cdot 5H_2O$ [a]

atom	m	p	x	y	z
Ru	4	1	0.36811 (2)	0.27788 (3)	0.000
N1	4	1	0.4451 (2)	0.4082 (3)	0.000
N2	4	1	0.2863 (2)	0.1386 (4)	0.000
N3	8	1	0.4285 (1)	0.1846 (2)	0.2106 (5)
N4	8	1	0.3037 (1)	0.3636 (2)	0.2139 (5)
C1	4	1	0.4263 (2)	0.5244 (4)	0.000
C2	4	1	0.5214 (2)	0.3869 (3)	0.000
Cl1	4	1	0.28002 (7)	0.1081 (1)	0.500
Cl2	8	0.5	0.1033 (1)	0.4052 (1)	0.4485 (4)
Cl3	4	0.5	0.4400 (1)	0.4273 (3)	0.500
O1	4	0.5	0.5201 (4)	0.3061 (7)	0.500
O2	4	0.5	0.3862 (4)	0.5246 (7)	0.500
O3	4	0.5	0.1373 (7)	0.334 (2)	0.000
O4	8	0.25	0.1390 (8)	0.264 (2)	0.074 (4)
O5	8	0.25	0.093 (1)	0.403 (2)	0.127 (6)

[a] Key: m, site multiplicity; p, population.

---

[10] Beattie, J. K.; Hush, N. S.; Taylor, P. R.; Raston, C. L.; White, A. H. *J. Chem. Soc., Dalton Trans.* **1977**, 1121.

Table V. Final Atomic Positional Parameters with Standard Deviations in Parentheses for $[II,III](tos)_5 \cdot 4H_2O$ at 100 K

atom	*x*	*y*	*z*	atom	*x*	*y*	*z*
Ru1	0.24805 (3)	0.00202 (3)	0.85031 (3)	S3	0.5363 (1)	0.2028 (1)	0.3034 (1)
N11	0.1063 (3)	0.0054 (3)	0.7980 (3)	O13	0.4290 (2)	0.2033 (2)	0.2708 (2)
N21	0.4005 (3)	−0.0040 (3)	0.8960 (3)	O23	0.6037 (3)	0.2014 (3)	0.2348 (2)
N31	0.2991 (4)	0.1530 (3)	0.8959 (3)	O33	0.5350 (3)	0.1268 (2)	0.3428 (2)
N41	0.1964 (4)	−0.1492 (3)	0.8093 (4)	C13	0.5883 (4)	0.3127 (4)	0.3905 (3)
N51	0.3017 (4)	−0.0065 (3)	0.7254 (3)	C23	0.5691 (4)	0.3204 (4)	0.4766 (4)
N61	0.2060 (4)	0.0082 (4)	0.9780 (3)	C33	0.6034 (4)	0.4083 (4)	0.5433 (4)
Ru2	−0.22613 (3)	−0.02593 (3)	0.62795 (3)	C43	0.6539 (4)	0.4899 (4)	0.5239 (4)
N12	−0.0905 (3)	−0.0108 (3)	0.7003 (3)	C53	0.6739 (5)	0.4791 (4)	0.4372 (4)
N22	−0.3722 (4)	−0.0372 (4)	0.5525 (3)	C63	0.6421 (4)	0.3912 (4)	0.3706 (4)
N32	−0.2663 (4)	−0.1761 (3)	0.6007 (3)	C73	0.6848 (7)	0.5860 (5)	0.5955 (5)
N42	−0.1895 (4)	0.1236 (3)	0.6542 (3)	S4	0.3769 (1)	0.2478 (1)	0.6633 (1)
N52	−0.2986 (4)	−0.0039 (3)	0.7435 (3)	O14	0.3249 (3)	0.1895 (2)	0.7137 (2)
N62	−0.1573 (4)	−0.0502 (3)	0.5078 (3)	O24	0.3038 (3)	0.2674 (3)	0.6026 (2)
C1	0.0973 (4)	0.0556 (3)	0.7389 (3)	O34	0.4553 (3)	0.2068 (2)	0.6164 (2)
C2	0.0142 (4)	−0.0471 (3)	0.8099 (3)	C14	0.4458 (4)	0.3589 (3)	0.7428 (3)
C3	−0.0801 (4)	−0.0542 (3)	0.7640 (3)	C24	0.4872 (4)	0.3622 (4)	0.8279 (3)
C4	0.0018 (4)	0.0464 (3)	0.6915 (3)	C34	0.5388 (4)	0.4503 (4)	0.8907 (4)
S1	−0.0386 (1)	0.2009 (1)	0.4560 (1)	C44	0.5525 (4)	0.5352 (4)	0.8695 (4)
O11	−0.0382 (3)	0.1414 (3)	0.5137 (3)	C54	0.5136 (4)	0.5300 (4)	0.7837 (4)
O21	−0.1383 (3)	0.1746 (2)	0.3972 (2)	C64	0.4591 (4)	0.4423 (4)	0.7203 (4)
O31	0.0509 (3)	0.2035 (3)	0.4083 (3)	C74	0.6043 (6)	0.6307 (5)	0.9416 (5)
C11	−0.0231 (4)	0.3188 (3)	0.5272 (3)	S5	0.3512 (1)	0.8022 (1)	0.0388 (1)
C21	0.0667 (4)	0.3617 (4)	0.5911 (4)	O15	0.4443 (3)	0.8171 (3)	0.1035 (3)
C31	0.0827 (4)	0.4555 (4)	0.6439 (4)	O25	0.2689 (4)	0.8364 (3)	0.0842 (3)
C41	0.0125 (4)	0.5081 (4)	0.6340 (4)	O35	0.3781 (4)	0.8474 (3)	−0.0293 (3)
C51	−0.0785 (4)	0.4644 (4)	0.5727 (4)	O45	0.306 (2)	0.796 (2)	0.119 (2)
C61	−0.0970 (4)	0.3695 (4)	0.5187 (3)	O55	0.304 (3)	0.837 (2)	−0.020 (2)
C71	0.0359 (6)	0.6135 (5)	0.6904 (5)	O65	0.456 (2)	0.801 (2)	0.038 (2)
S2	0.9277 (1)	0.7880 (1)	0.9508 (1)	C15	0.3020 (4)	0.6779 (4)	−0.0171 (4)
O12	0.9046 (3)	0.7974 (2)	1.0417 (2)	C25	0.2498 (4)	0.6186 (4)	0.0260 (4)
O22	1.0390 (3)	0.8295 (2)	0.9508 (2)	C35	0.2139 (5)	0.5206 (4)	−0.0166 (4)
O32	0.8571 (3)	0.8221 (2)	0.9013 (2)	C45	0.2293 (4)	0.4803 (4)	−0.1045 (4)
C12	0.9054 (4)	0.6639 (4)	0.8938 (3)	C55	0.2817 (4)	0.5401 (4)	−0.1466 (4)
C22	0.9794 (4)	0.6165 (4)	0.9129 (4)	C65	0.3176 (4)	0.6386 (4)	−0.1050 (4)
C32	0.9614 (5)	0.5183 (4)	0.8667 (4)	C75	0.1873 (6)	0.3753 (5)	−0.1524 (5)
C42	0.8713 (4)	0.4689 (4)	0.8043 (4)	O1	0.6803 (3)	0.1293 (3)	0.4862 (3)
C52	0.7994 (4)	0.5170 (4)	0.7873 (4)	O2	0.0873 (3)	0.8087 (4)	0.1558 (3)
C62	0.8159 (4)	0.6146 (4)	0.8309 (5)	O3	0.4113 (4)	0.8642 (3)	0.2887 (3)
C72	0.8542 (6)	0.3627 (5)	0.7551 (4)	O4	0.4148 (3)	0.1432 (3)	0.0765 (3)

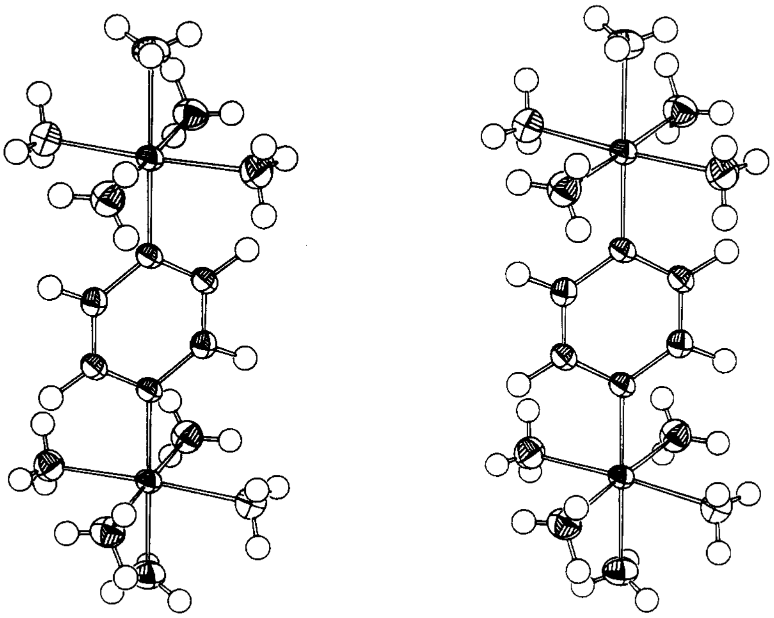

Figure 1. Stereoview of $[(NH_3)_5Ru(pyz)Ru(NH_3)_5]^{5+}$ in the crystal structure of $[II,III]Cl_5 \cdot 5H_2O$.

deviates from the pyrazine least-squares plane by 0.001, 0.326, and 0.029 Å for $[II,II](ZnCl_4)_2$, $[II,III](tos)_5 \cdot 4H_2O$, and $[III,III]Cl_6 \cdot 2H_2O$, respectively.

Structural Data and Mixed-Valence Properties

The survey of distances and angles summarized in Table VII shows only rather subtle changes along the electron-transfer series. The smallest shifts occur for the *cis*-Ru–NH_3 bond lengths where the dependence of the distance on the oxidation states closely follows the trend observed for corresponding mononuclear ruthenium amines.[11] More pronounced and significant differences

---

(11) Stynes, H. C.; Ibers, J. A. *Inorg. Chem.* **1971**, *10*, 2304. Richardson, D. E.; Walker, D. D.; Sutton, J. E.; Hodgson, K. O.; Taube, H. *Ibid.* **1979**, *18*, 2216. Gress, M. E.; Creutz, C.; Quicksall, C. O. *Ibid.* **1981**, *20*, 1522.

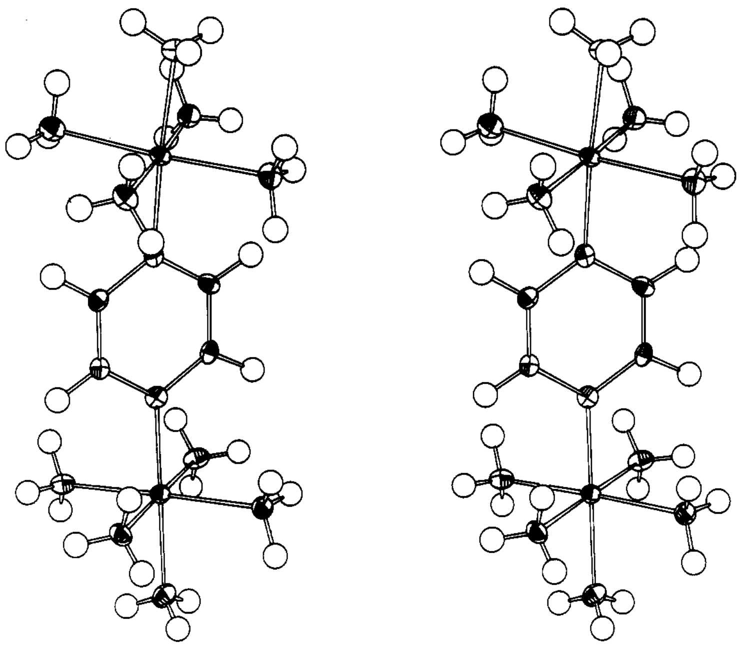

Figure 2. Stereoview of $[(NH_3)_5Ru(pyz)Ru(NH_3)_5]^{5+}$ in the crystal structure of [II,III](tos)$_5$·4H_2O.

Table VI. Final Atomic Positional Parameters with Standard Deviations in Parentheses for [III,III]Cl_6·2H_2O

atom	x	y	z
Ru	0.21645 (2)	0.26031 (1)	0.08620 (1)
N1	0.0865 (2)	0.4036 (2)	0.0334 (1)
N2	0.3458 (3)	0.1213 (2)	0.1409 (1)
N3	0.1784 (3)	0.3346 (2)	0.2199 (1)
N4	0.2663 (3)	0.1766 (2)	−0.0452 (1)
N5	−0.0303 (3)	0.1705 (2)	0.1227 (1)
N6	0.4717 (2)	0.3409 (2)	0.0502 (1)
C1	0.1204 (3)	0.5147 (2)	0.0552 (2)
C2	−0.0355 (3)	0.3901 (2)	−0.0228 (2)
Cl1	0.6052 (1)	0.27020 (6)	0.25817 (5)
Cl2	0.51405 (9)	0.41535 (5)	0.83264 (4)
Cl3	0.23141 (5)	0.38776 (5)	0.46752 (5)
O1	0.1350 (3)	0.5114 (2)	0.7440 (2)

are observed for the Ru–NH_3(trans) bond and the Ru–N(pyz) distances.

The salient structural result emerging from our crystallographic study of the complete electron-transfer series is an unequivocal demonstration that the structure of the mixed-valence ion is not midway between the completely oxidized and reduced forms (Table VIII). This precludes interpretations of the symmetric [II,III] structure in terms of two disordered asymmetric ions, each with one Ru(II) and one Ru(III) center resembling those of [II,II], [III,III] (Table VIII), or the corresponding monomers.[11] The differences between the Ru–N(pyz) and *trans*-Ru–NH_3 distances, particularly for [II,II] and [II,III], present clear evidence for a strong electronic interaction between Ru and the pyrazine bridge. The t_{2g}–π^* back-bonding is also reflected in the geometry of the pyrazine molecule. For [II,II] and [II,III], lengthening of the

Table VII. Symmetry and Selected Interatomic Distances (Å) and Angles (deg) for $[(NH_3)_5Ru(pyz)Ru(NH_3)_5]^{n+}$ (n = 4–6)

	[II,II]	[II,III]Cl_5	[II,III](tos)$_5$[a]		[III,III]
		Symmetry			
	$\bar{1}$	$2/m$	1		$\bar{1}$
		Distances			
Ru-Ru	6.877 (1)	6.840 (1)	6.781 (1)		7.043 (1)
Ru-N1(pyz)	2.013 (3)	2.002 (2)	1.998 (4)	1.972 (4)	2.115 (1)
Ru-N2(trans)	2.149 (3)	2.134 (3)	2.109 (5)	2.126 (5)	2.089 (1)
Ru-N3	2.137 (4)	2.105 (3)	2.114 (5)	2.108 (5)	2.101 (1)
Ru-N4	2.133 (3)	2.117 (3)	2.108 (4)	2.113 (5)	2.116 (2)
Ru-N5	2.131 (3)		2.119 (5)	2.095 (5)	2.091 (2)
Ru-N6	2.125 (3)		2.108 (5)	2.132 (5)	2.095 (2)
Ru-N(cis)[b]	2.132 (3)	2.111 (3)	2.112 (3)	2.112 (8)	2.101 (5)
N1-C1[c]	1.349 (4)	1.355 (4)	1.376 (8)	1.364 (6)	1.341 (2)
N1-C2[c]	1.356 (4)	1.364 (4)	1.348 (6)	1.363 (7)	1.341 (2)
C1-C4[c]	1.363 (5)	1.361 (4)	1.369 (7)	1.353 (7)	1.382 (2)
		Angles			
N1-Ru-N2	178.2 (2)	179.9 (1)	175.8 (2)	178.0 (2)	178.7 (1)
N1-Ru-N3	90.0 (2)	91.6 (1)	91.2 (2)	91.6 (2)	92.0 (1)
N1-Ru-N4	90.0 (1)	91.4 (1)	89.4 (2)	89.6 (2)	92.0 (1)
N1-Ru-N5	91.0 (1)		90.1 (2)	90.5 (2)	91.7 (1)
N1-Ru-N6	92.1 (1)		94.5 (2)	91.3 (2)	91.5 (1)
C2-N1-C1	113.3 (3)	114.3 (3)	115.1 (4)	114.0 (4)	115.6 (1)
N1-C1-C4	123.0 (3)	123.3 (3)	121.5 (4)	123.2 (5)	122.9 (2)
N1-C2-C3	123.7 (3)	122.4 (3)	122.9 (5)	123.1 (5)	121.6 (2)

[a] 100 K. [b] Average; $\sigma(\mathrm{av}) = [\Sigma^{\mathrm{m}}(\bar{x} - x_i)^2/m(m-1)]^{1/2}$. [c] Free pyrazine: C–N = 1.333 (1), C–C = 1.388 (1) Å; C–N–C = 116.2 (1), C–C–N = 121.9 (1)°; 184 K; R = 7.1%. De With, G.; Harkema, S.; Feil, D. *Acta Crystallogr., Sect. B: Struct. Crystallogr. Cryst. Chem.* **1976**, *B32*, 3178.

Table VIII. Average Distances[a] (Å) for $[(NH_3)_5Ru(pyz)Ru(NH_3)_5]^{n+}$ (n = 4–6)

	n = 4 [II,II]	n = 5 [II,III]	n = 6 [III,III]
Ru-N(pyz)	2.013 (3)	1.991 (9)	2.115 (1)
Ru-N(trans)	2.149 (3)	2.123 (7)	2.089 (1)
Ru-N(cis)	2.132 (3)	2.112 (3)	2.101 (5)
C-N	1.353 (4)	1.362 (4)	1.341 (2)
C-C	1.363 (5)	1.361 (5)	1.382 (2)

[a] See footnotes *b* and *c* of Table VII.

C–N bond and contraction of the C–C bonds are observed, in agreement with the transfer of electron density from the t_{2g}(Ru) subshell into the LUMO of pyrazine.[12a] Since the mixed-valence interaction between the two metal centers is obviously mediated by the bridging ligand, its electronic structure has to be considered explicitly in a thorough discussion of the Creutz–Taube ion. C–N and C–C distances for [III,III] do not show signs of back-donation; they are very close to the values of free pyrazine.

The structural results for [II,III]$Cl_5 \cdot 5H_2O$—two equivalent ruthenium atoms—and [II,III]$(tos)_5 \cdot 4H_2O$—two distinct ruthenium atoms—appear to be in conflict with each other. However, the difference in the Ru–N1(pyz) distances (0.026 Å) of the tosylate is small compared to the difference (0.102 Å) observed between [II,II] and [III,III]. The same observation applies to Ru–N2(trans) (0.017 Å vs. 0.06 Å) and to the average Ru–N(cis) bonds (0.000 Å vs. 0.031 Å). There are two possible interpretations of these data: (i) The isolated [II,III] ion is symmetric. Discussion of the rather subtle structural differences between the [II,III] dimers in the two salts would have to resort to the different temperatures of the diffraction experiments, room temperature for the chloride and 100 K for the tosylate. Moreover, packing forces, in particular the hydrogen-bond network, could affect details of the molecular structure in a complex and unpredictable manner. (ii) The isolated [II,III] ion is asymmetric, its ground state being described by a double-well potential with two equivalent minima; upon packing [II,III] is trapped in one of the two minima with an asymmetric molecular geometry. If this were the case, the two Ru atoms would still be far from being Ru(II) and Ru(III) ions as in [II,II] or [III,III] or the corresponding monomers. The observed centrosymmetric structure of [II,III]$Cl_5 \cdot 5H_2O$ would not have to be in disagreement with this view provided the two asymmetric [II,III] ions show static or dynamic disorder. Such a disorder would affect the differences in temperature factors along the Ru–N bonds ($\Delta U \sim \Delta d^2$(Ru–N)/4);[13] as estimated from the [II,III] tosylate, the effect would be on the order of 4×10^{-5} Å^2, far too small to be observable in our study where esd's of temperature factors for nitrogen are about 0.002 Å^2. As a consequence of the small differences between the coordination geometries of ruthenium, the barrier between the two minima would be very small too, on the order of vibrational energies, and therefore very difficult to determine reliably.

In view of the above discussion it is impossible to decide whether the difference in the molecular structure for the two [II,III] salts is due to an intrinsic property of the binuclear mixed-valence ion or largely due to crystal packing. Because of our inability to distinguish unambiguously between (i) and (ii) we prefer the simplest possible description, namely (i), i.e., a symmetric [II,III] ion with normal vibrational behavior and without a double-well potential. In any case, the structural results for the *complete* electron-transfer series conclusively demonstrate that the mixed-valence ion is not a combination of genuine Ru(II) and Ru(III) moieties. In addition they clearly reveal the importance of the metal–ligand interaction for strongly coupled mixed-valence compounds. A more detailed discussion of the electronic structure of the Creutx–Taube ion based on a variety of spectroscopic data and model calculations will be given in two subsequent papers.[12]

Acknowledgment. We thank Dr. H. Wagner, CIBA Geigy, Basel, for the elemental analyses. This work was supported by the Swiss National Science Foundation (Grant No. 2.209-0.81).

Registry No. [II,II]$(ZnCl_4)_2$, 87922-19-8; [III,III]$Cl_6 \cdot 2H_2O$, 87922-22-3; [II,III]$Cl_5 \cdot 5H_2O$, 87922-20-1; [II,III]$(tos)_5 \cdot 4H_2O$, 87922-21-2; $[Ru(NH_3)_5Cl]Cl_2$, 18532-87-1.

Supplementary Material Available: Listings of structure factors, thermal parameters, hydrogen positions, and bond lengths and angles for the anions of [II,III]$(ZnCl_4)_2$, [II,III]$Cl_5 \cdot 5H_2O$, [II,III]$(tos)_5 \cdot 4H_2O$, and [III,III]$Cl_6 \cdot 2H_2O$ and stereoviews of the unit cells for [II,II]$(ZnCl_4)_2$, [II,III]$(tos)_5 \cdot 4H_2O$, and [III,III]$Cl_6 \cdot 2H_2O$ (72 pages). Ordering information is given on any current masthead page.

---

[12] (a) Joss, S.; Bürgi, H. B.; Ludi, A., submitted for publication. (b) Joss, S.; Fürholz, U.; Hasselbach, K. M.; Bürgi, H. B.; Wordel, R.; Wagner, F. E.; Ludi, A., to be submitted for publication.

[13] Chandrasekhar, K.; Bürgi, H. B. *Acta Crystallogr., Sect. B: Struct. Sci.* **1984**, *B40*, 387.